Donor–Acceptor Conjugated Polymers with Dithienocarbazoles as Donor Units: Effect of Structure on Semiconducting Properties

ARTICLE *in* MACROMOLECULES · NOVEMBER 2012

Impact Factor: 5.8 · DOI: 10.1021/ma301864f

8 AUTHORS, INCLUDING:

Yunfeng Deng
Chinese Academy of Sciences
10 PUBLICATIONS **165** CITATIONS
SEE PROFILE

Yagang Chen
Chinese Academy of Sciences
7 PUBLICATIONS **106** CITATIONS
SEE PROFILE

Hongkun Tian
Chinese Academy of Sciences
88 PUBLICATIONS **1,431** CITATIONS
SEE PROFILE

Macromolecules

Article

pubs.acs.org/Macromolecules

Donor–Acceptor Conjugated Polymers with Dithienocarbazoles as Donor Units: Effect of Structure on Semiconducting Properties

Yunfeng Deng,[†,‡] Yagang Chen,[†,‡] Xiaojie Zhang,*[,†] Hongkun Tian,[†] Cheng Bao,[†] Donghang Yan,[†] Yanhou Geng,*[,†] and Fosong Wang[†]

[†]State Key Laboratory of Polymer Physics and Chemistry, Changchun Institute of Applied Chemistry, Chinese Academy of Sciences, Changchun 130022, P. R. China

[‡]University of Chinese Academy of Sciences, Beijing 100049, P. R. China

Supporting Information

ABSTRACT: A series of donor–acceptor (D–A) conjugated polymers (CPs) comprising dithieno[2,3-*b*;7,6-*b*]carbazole (**C1**) or dithieno[3,2-*b*;6,7-*b*]carbazole (**C2**) as D unit and thienopyrroledione (**TPD**), isoindigo (**IID**), or diketopyrrolopyrrole (**DPP**) as A unit were synthesized, and their semiconducting properties were investigated with organic field-effect transistors (OFETs). Because of different bonding geometry of **C1** and **C2**, the CPs based on these isomeric D units have distinct backbone conformation. The CPs based on **C1** unit and all three A units show strong backbone curvature. In consequence, these polymers all formed amorphous films and exhibited low OFET mobility in the level of 10^{-3} $cm^2/(V\ s)$. **P(TPD-C2)** and **P(DPP-C2)**, which comprise **C2** and **TPD** or **DPP**, both display pseudo-straight-shaped backbones and formed ordered films with the polymer backbones adopting edge-on orientation respective to the substrates. Accordingly, **P(TPD-C2)** and **P(DPP-C2)** exhibited the highest mobility of 0.31 and 1.36 $cm^2/(V\ s)$, respectively. However, **P(IID-C2)** could only form amorphous films probably owing to its highly stiff backbone, leading to a moderate OFET mobility (2.96×10^{-2} $cm^2/(V\ s)$). This implies that large fused aromatics are promising building blocks for high-mobility D–A CPs when polymer backbone conformation and rigidity are appropriately manipulated.

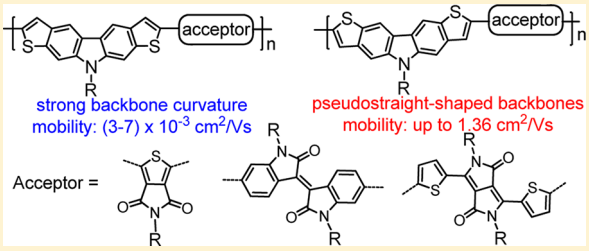

INTRODUCTION

Organic field-effect transistors (OFETs) are receiving increasing attention due to their potential applications in display technologies, smart cards, and radio-frequency identification (RFID) tags.[1−5] Developing high mobility organic/polymeric semiconductors is crucial to improve the performance of OFETs toward the requirements of aforementioned applications. In this regard, solution processable π-conjugated polymers (CPs) are of particularly interest compared to small molecular counterparts because of their tunable solution rheological properties, which enable proper ink formulations for high-throughput printing processes on large-area, lightweight, and flexible substrates.[6−9]

To date, two molecular design concepts have been proposed for designing high mobility CPs. One is incorporating multifused heteroarenes into polythiophene backbone to enhance the coplanarity and thus the intermolecular interaction.[10−24] Based on this concept, various CPs have been developed, and the OFET mobility as high as 0.77 $cm^2/(V\ s)$ has been achieved.[21] Another protocol is alternatively linking electron-rich and electron-deficient aromatic units to form donor–acceptor (D–A) CPs.[25−59] This type of CP is characterized with strong intermolecular interactions induced by the large dipole moment between D and A units and therefore often exhibits high OFET mobility. For instance, Müllen et al. found that high molecular weight poly(cyclopentadithiophene-*co*-benzothiadiazole) exhibited OFET mobility up to 5.5 $cm^2/(V\ s)$.[40−42] Li et al. and other groups reported a series of D–A CPs based on diketopyrrolopyrrole (**DPP**) which exhibited mobility up to 2.2 $cm^2/(V\ s)$.[43−55] Recently, Liu et al. found that the mobility of **DPP** based D–A CPs could be further enhanced to 8 $cm^2/(V\ s)$ upon optimizing the structure of D-unit.[56] Pei et al. first reported isoindigo (**IID**) based D–A CPs with mobility up to 1.06 $cm^2/(V\ s)$.[57,58] Later, Bao et al. optimized the structures of solubilizing groups in **IID** unit for shortening π–π stacking distance. As a result, OFET mobility up to 2.48 $cm^2/(V\ s)$ was realized.[59]

According to the aforementioned achievements, D–A CPs comprising large heteroacenes as D-units, which combine the structural features of aforementioned two types of high mobility CPs, should be attractive as high mobility semiconductors because coplanar geometries and rigid structures of the heteroacene units can suppress rotational disorder around interannular single bonds and lower the reorganization energy, leading to even stronger intermolecular interaction. However, the incorporation of large heteroarenes into D–A CPs will also cause the decrease of solubility due to the strong intermolecular interaction.[20] Recently, we have synthesized two novel

Received: September 6, 2012
Revised: October 11, 2012

   dx.doi.org/10.1021/ma301864f | *Macromolecules* XXXX, XXX, XXX–XXX

heteroacenes containing five fused rings, i.e., dithieno[2,3-*b*;7,6-*b*]carbazole (**C1**) and dithieno[3,2-*b*;6,7-*b*]carbazole (**C2**),[23,24] which allow introducing an additional alkyl chain on N atom for improving the solubility of CPs. Therefore, in the current paper, we designed and synthesized six D−A CPs based on these two heteroacene units and three A units, i.e., thienopyrroledione (**TPD**), **IID**, and **DPP** which have been widely used in the design of D−A CPs, and their photophysical and semiconducting properties were studied in detail to explore the effect of the chemical structures on their properties.

RESULTS AND DISCUSSION

Synthesis. D−A CPs **P(TPD-C1)**, **P(TPD-C2)**, **P(IID-C1)**, **P(IID-C2)**, **P(DPP-C1)**, and **P(DPP-C2)** as shown in Scheme 1 were synthesized by typical Stille cross-coupling

Scheme 1. Chemical Structures and Synthetic Route to the Polymers

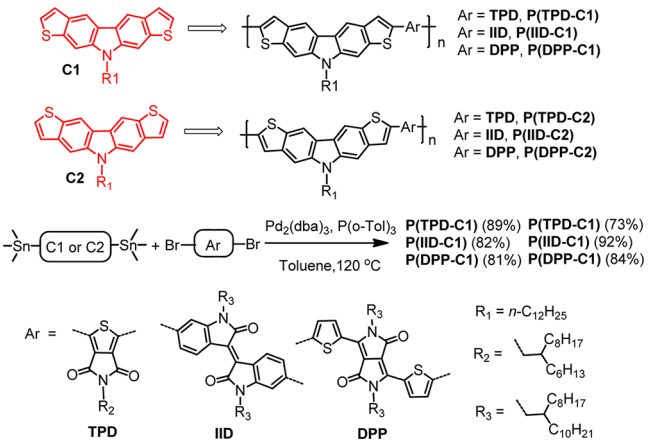

polycondensation in high yields.[23,24] The resulting polymers were purified by multiprecipitation and Sohxlet extraction with acetone, hexane, and chloroform in succession. The molecular weights of the polymers were measured by gel-permeation chromatography (GPC) with polystyrene as standard, and the results are listed in Table 1. All polymers showed good solubility in common organic solvents, such as chloroform and dichlorobenzene.

Table 1. Number-Average Molecular Weights (M_n), Weight-Average Molecular Weights (M_w), Polydispersity Indices (PDI), and Thermal Decomposition Temperatures (T_d) of the Polymers

polymers	M_n (kDa)[a]	M_w (kDa)[a]	PDI[a]	T_d (°C)[b]
P(TPD-C1)	30.8	55.3	1.8	412
P(TPD-C2)	12.2	17.5	1.4	378
P(IID-C1)	20.1	54.3	2.7	403
P(IID-C2)	17.2	38.9	2.3	406
P(DPP-C1)	18.8	46.3	2.5	400
P(DPP-C2)	89.9	146.1	1.7	387

[a]Molecular weights and PDIs of **P(TPD-C1)** and **P(TPD-C2)** were measured by GPC at 40 °C with tetrahydrofuran as eluent and polystyrene as standard, while those of **P(IID-C1)**, **P(IID-C2)**, **P(DPP-C1)**, and **P(DPP-C2)** were measured by GPC at 150 °C with 1,2,4-trichlorobenzene as eluent and polystyrene as standard. [b]Reported as the temperature with 5% weight loss.

Thermal Properties. Thermal stability was evaluated by thermogravimetric analysis (TGA) in nitrogen with a heating rate of 10 °C/min. As shown in Figure 1, all the polymers are

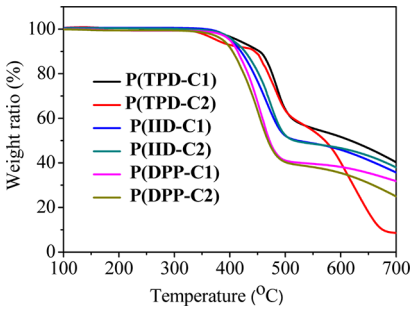

Figure 1. TGA plots of the polymers with a heating rate of 10 °C/min in a N_2 atmosphere.

thermally stable with decomposition temperatures (T_d) above 380 °C (Table 1). Differential scanning calorimetry (DSC) analysis was also performed in nitrogen with a heating/cooling rate of ±10 °C/min (shown in Figure S1of the Supporting Information), and no obvious thermal transitions were observed before decomposition for all polymers. This phenomenon was also observed for other high mobility CPs.[58−62]

Photophysical and Electrochemical Properties. Figure 2 displays solution and film absorption spectra of polymers

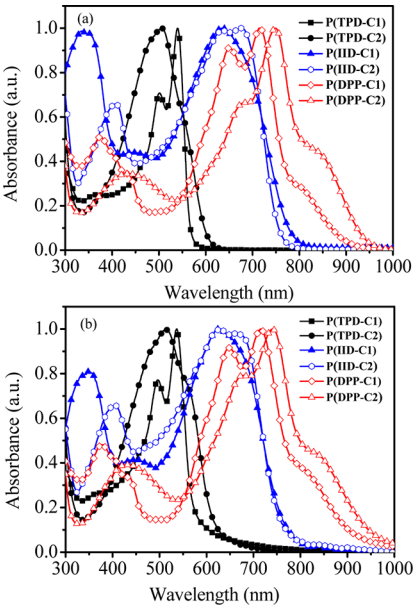

Figure 2. Solution (a) and film (b) UV−vis−NIR absorption spectra of the polymers. Solution spectra were measured in chlorobenzene with a concentration of 10^{-5} mol/L of repeating units. Films with a thickness of ∼45 nm were prepared by spin-casting the dichlorobenzene solutions with a concentration of 6 mg/mL on quartz substrates.

P(TPD-C1), **P(TPD-C2)**, **P(IID-C1)**, **P(IID-C2)**, **P(DPP-C1)**, and **P(DPP-C2)**, and the related data are summarized in Table 2. In dilute solutions, **P(TPD-C1)** and **P(TPD-C2)** showed one absorption band with maxima at 540 and 507 nm, respectively. **P(IID-C1)**, **P(IID-C2)**, **P(DPP-C1)**, and **P(DPP-C2)** exhibited two major absorption bands in dilute solutions.

dx.doi.org/10.1021/ma301864f | *Macromolecules* XXXX, XXX, XXX−XXX

Table 2. Optical and Electrochemical Properties of the Polymers

polymer	λ_{max} (nm) solution[a]	λ_{max} (nm) film	E_g^{opt} (eV)[b]	E_{onset}^{ox} (V)	E_{onset}^{re} (V)	HOMO[c] (eV)	LUMO (eV)[c]	E_g^{cv} (eV)[d]
P(TPD-C1)	501, 540	499, 535	2.05	0.50	−1.98	−5.30	−2.82	2.48
P(TPD-C2)	507, 543	516, 556	1.98	0.48	−1.93	−5.28	−2.87	2.41
P(IID-C1)	339, 637	349, 635	1.60	0.40	−1.26	−5.20	−3.54	1.66
P(IID-C2)	405, 679	407, 675	1.61	0.42	−1.26	−5.22	−3.54	1.68
P(DPP-C1)	372, 648, 719	376, 647, 718	1.35	0.32	−1.39	−5.12	−3.41	1.71
P(DPP-C2)	434, 685, 748	434, 684, 745	1.31	0.33	−1.41	−5.13	−3.39	1.74

[a]Measured in chlorobenzene with a concentration of 10^{-5} mol/L of the repeating units. [b]Optical bandgap (E_g^{opt}) was calculated from the film absorption onset. [c]The highest occupied molecular orbital (HOMO) and the lowest unoccupied molecular orbital (LUMO) energies were calculated according to HOMO = $-(4.80 + E_{onset}^{ox})$ eV and LUMO = $-(4.80 + E_{onset}^{re})$ eV, in which E_{onset}^{ox} and E_{onset}^{re} represent oxidation and reduction onset potentials, respectively. [d]Calculated according to E_g^{cv} = LUMO − HOMO.

The shorter wavelength absorption bands at 339, 405, 372, and 434 nm for **P(IID-C1)**, **P(IID-C2)**, **P(DPP-C1)**, and **P(DPP-C2)**, respectively, are originated from the $\pi-\pi^*$ transition, while the longer wavelength ones at 637, 649, 719, and 748 nm for **P(IID-C1)**, **P(IID-C2)**, **P(DPP-C1)**, and **P(DPP-C2)**, respectively, are attributed to the intramolecular charge transfer (ICT) between D and A units. Compared with **C1**-containing polymers **P(IID-C1)** and **P(DPP-C1)**, the absorption maxima of the polymers **P(IID-C2)** and **P(DPP-C2)**, which comprise **C2** as donor unit, exhibited a noticeable red-shift. This indicates that the polymers based on **C2** unit have more extended conjugation. The film absorption spectra of the polymers as shown in Figure 2b are identical to those in solutions, even after annealing the film at 150 °C for 20 min (Figure S2). Optical bandgaps (E_g^{opt}) deduced from the absorption edges of the film spectra are in the following order: **P(TPD-C1)** (2.05 eV) > **P(TPD-C2)** (1.98 eV) > **P(IID-C1)** (1.60 eV) ~ **P(IID-C2)** (1.61 eV) > **P(DPP-C1)** (1.35 eV) ~ **P(DPP-C2)** (1.31 eV).

Thin film cyclic voltammentry (CV) was employed to investigate the electrochemical property and determine the highest occupied molecular orbital (HOMO) and the lowest unoccupied molecular orbital (LUMO) energy levels of the polymers. As shown in Figure 3, all polymers showed both p- and n-doping processes. Reversible or quasi-reversible n-doping processes were observed for all polymers except **P(TPD-C1)**. The polymers based on **C1** exhibited reversible or quasi-reversible p-doping processes while the polymers based on **C2** showed irreversible p-doping processes. Asymmetric voltammograms or irreversible redox processes are often observed for conjugated polymer films, and the common explain is that the dedoping reaction cannot be regarded as just the reverse reaction of the doping process.[63] For example, charge ejection from the film, which is involved in the dedoping process, usually takes place in a broad potential interval, resulting in a delayed dedoping peak. The oxidation and reduction onset potentials (E_{onset}^{ox} and E_{onset}^{re}, respectively) of the polymers versus Fc/Fc^+ are listed in Table 2. The HOMO and LUMO energy levels were calculated according to the equations HOMO = $-(4.80 + E_{onset}^{ox})$ eV and LUMO = $-(4.80 + E_{onset}^{re})$,[64] which were estimated to be −5.30 and −2.82 eV for **P(TPD-C1)**, −5.28 and −2.87 eV for **P(TPD-C2)**, −5.20 and −3.54 eV for **P(IID-C1)**, −5.22 and −3.54 eV for **P(IID-C2)**, −5.12 and −3.41 eV for **P(DPP-C1)**, and −5.13 and −3.39 eV for **P(DPP-C2)**. Note that the polymers based on **C1** and **C2** with the same A unit have identical HOMO energy levels, indicating that these two isomeric units have similar electron-donating strength. Electrochemical bandgaps of the polymers (E_g^{cv}) were also calculated based on HOMO and LUMO energy levels, which showed a trend similar to E_g^{opt} deduced from absorption onsets.

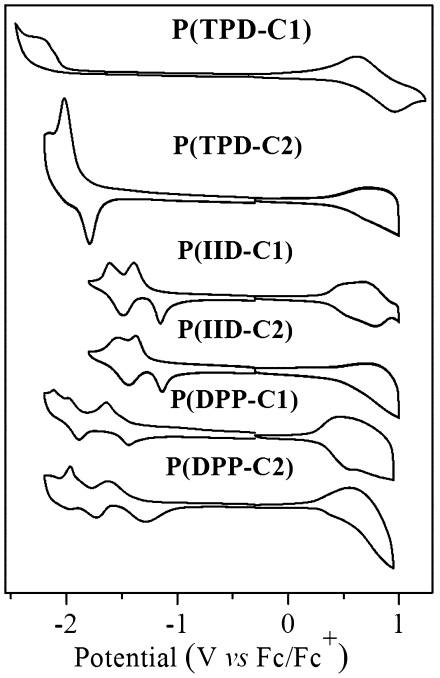

Figure 3. Thin film cyclic voltammograms of the polymers. The measurements were conducted in acetonitrile at a scan rate of 100 mV/s with Bu_4NPF_6 (0.1 mol/L) as electrolyte. The films of ~45 nm were prepared by spin-casting dichlorobenzene solutions on the working electrode.

OFET Properties. OFET devices were fabricated with a top contact and bottom gate geometry to investigate the semiconducting properties of the polymers. The device characteristics were measured in ambient atmosphere. All the devices showed typical p-channel characteristics, and mobility was calculated from saturation regime. Figure 4 shows typical output and transfer curves of the devices based on **P(TPD-C2)** and **P(DPP-C2)**. Table 3 summarizes the performance data of the devices based on pristine films and the films after thermal annealing at optimized temperatures. Clearly, the structures of both D and A units significantly affect the semiconducting properties of the polymers. Devices from the pristine films of **P(TPD-C2)**, **P(IID-C2)**, and **P(DPP-C2)** exhibited mobilities up to 0.20, 5.50×10^{-3}, and 0.45 $cm^2/(V\ s)$, respectively. Thermal annealing of the films resulted in a significant improvement of device performance, although no phase

dx.doi.org/10.1021/ma301864f | Macromolecules XXXX, XXX, XXX−XXX

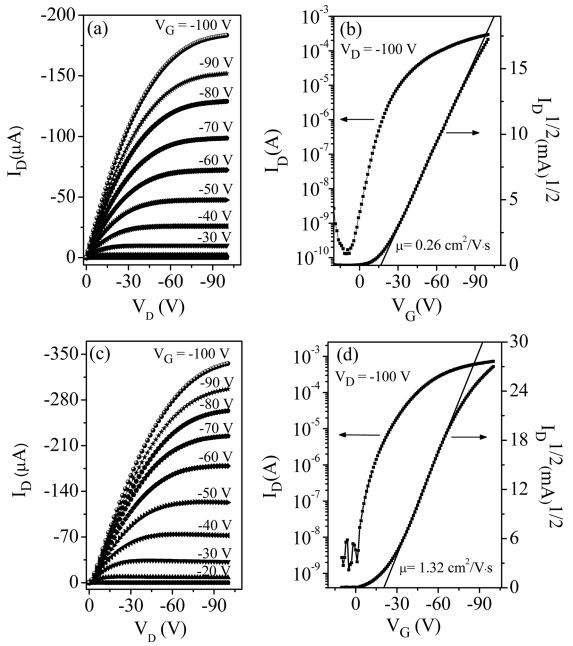

Figure 4. Typical output (a, c) and transfer (b, d) characteristics of OFET devices of **P(TPD-C2)** (a, b) and **P(DPP-C2)** (c, d). The films were spin-casting from dichlorobenzene solutions and annealed for 20 min. The annealing temperatures of the films are 150 and 200 °C, respectively.

transitions were observed in DSC measurements for all polymers. Mobilities up to 0.31, 2.96 × 10^{-2}, and 1.36 cm^2/(V s) for **P(TPD-C2)**, **P(IID-C2)**, and **P(DPP-C2)**, respectively, were achieved. A recent study by Pei et al. revealed that D−A CPs comprising axisymmetric D-units had mobility <0.1 cm^2/(V s), much lower than those based on centrosymmetric D-units.[58] They attributed this phenomenon to the poorer "molecular docking" ability of the polymers based on axisymmetric D-units. The **C2** unit is a typical axisymmetric unit, but mobilities of **P(TPD-C2)** and **P(DPP-C2)** (0.31 and 1.36 cm^2/(V s), respectively) are higher than those of **TPD**- and **DPP**-based D−A CPs containing a centrosymmetric bithiophene D-unit (0.19 and 0.97 cm^2/(V s), respectively[34,44]). These results clearly indicate the positive effect of large heteroacenes on semiconducting properties of D−A CPs upon appropriate molecular design. Moreover, the mobility of **P(DPP-C2)** is about triple that of the polymer based on **C2** and bithiophene unit,[24] further proving the advantages of D−A CPs in terms of charge transport properties. In contrast, **C1**-containing polymers **P(TPD-C1)**, **P(IID-C1)**, and **P(DPP-C1)** all showed OFET mobilities in the magnitude of 10^{-3} cm^2/(V s), even after the films were thermally annealed. Their mobilities are even lower than those of CPs comprising **C1** and bithiophene units.[23] Note that the slopes of the $(I_D)^{1/2}$ vs V_G curves started to drop at high V_G for the devices based on **P(DPP-C1)**, **P(DPP-C2)**, and **P(IID-C1)** (Figure 4d, Figures S3d and Figure S3h). This phenomenon was also observed for other **DPP**-based polymers[44,45,53,56] and may be attributed to the contact resistance between the semiconductor and the source/drain electrodes.

Ordering structures of the polymer films on octylsilyl trichloride (OTS)-modified Si/SO_2 substrates were studied by thin film X-ray diffraction (XRD) and selected area electron diffraction (SAED). As shown in Figure 5 and Figure S4, no

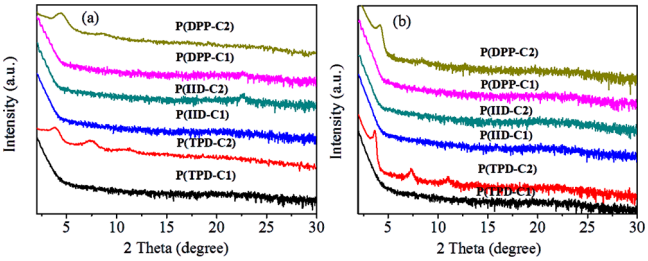

Figure 5. Thin film XRD patterns of the polymer pristine films (a) and those after thermally annealed for 20 min (b). The films with the thickness of ~50 nm were prepared by spin-casting on OTS-treated Si/SiO_2 substrates with *o*-DCB as the solvent. Annealing was conducted at 150 °C for **P(TPD-C1)**, **P(TPD-C2)**, and **P(DPP-C1)**, 200 °C for **P(DPP-C2)**, and 250 °C for **P(IID-C1)** and **P(IID-C2)**.

clear diffraction peaks were observed in both XRD and SAED patterns of **P(TPD-C1)**, **P(IID-C1)**, **P(IID-C2)**, and **P(DPP-C1)** films even after thermal annealing. This implies amorphous nature of the films and is consistent with the low device mobility of these polymers. The pristine films of **P(TPD-C2)** and **P(DPP-C2)** showed diffraction peaks up to the third and second orders with the (100) peaks at 2θ = 3.93° and 4.43°, respectively, corresponding to the *d*-spacing values of 22.5 and

Table 3. OFET Device Performance of the Polymers[a]

polymer	annealing temp	μ_{max} (cm^2/(V s))[a]	μ_{ave} (cm^2/(V s))[a]	V_T (V)[b]	I_{on}/I_{off}[c]
P(TPD-C1)	pristine	7.0 × 10^{-4}	6.1 × 10^{-4}	−7.2 to −4.82	~10^3
	150 °C	2.9 × 10^{-3}	2.6 × 10^{-3}	−17.0 to −11.2	~10^4
P(TPD-C2)	pristine	0.20	0.12	−4.2 to 1.6	~10^5
	150 °C	0.31	0.24	−18.3 to −14.5	~10^6
P(IID-C1)	pristine	1.3 × 10^{-3}	9.7 × 10^{-4}	−8.65 to −3.23	~10^4
	250 °C	3.1 × 10^{-3}	2.5 × 10^{-3}	−11.7 to −8.7	~10^4
P(IID-C2)	pristine	5.5 × 10^{-3}	4.2 × 10^{-3}	−24.3 to −21.1	~10^4
	250 °C	2.96 × 10^{-2}	2.4 × 10^{-2}	−26.5 to −23.8	~10^5
P(DPP-C1)	pristine	3.8 × 10^{-3}	3.6 × 10^{-3}	−3.6 to 0.16	~10^3
	150 °C	6.7 × 10^{-3}	5.4 × 10^{-3}	−2.4 to 0.64	~10^4
P(DPP-C2)	pristine	0.45	0.34	−17.1 to −14.4	~10^5
	200 °C	1.36	1.10	−22.4 to −13.7	~10^5

[a]Mobility calculated from saturation region, and average mobility was calculated from more than five parallel devices. [b]Threshold voltage. [c]Current on/off ratio.

dx.doi.org/10.1021/ma301864f | *Macromolecules* XXXX, XXX, XXX−XXX

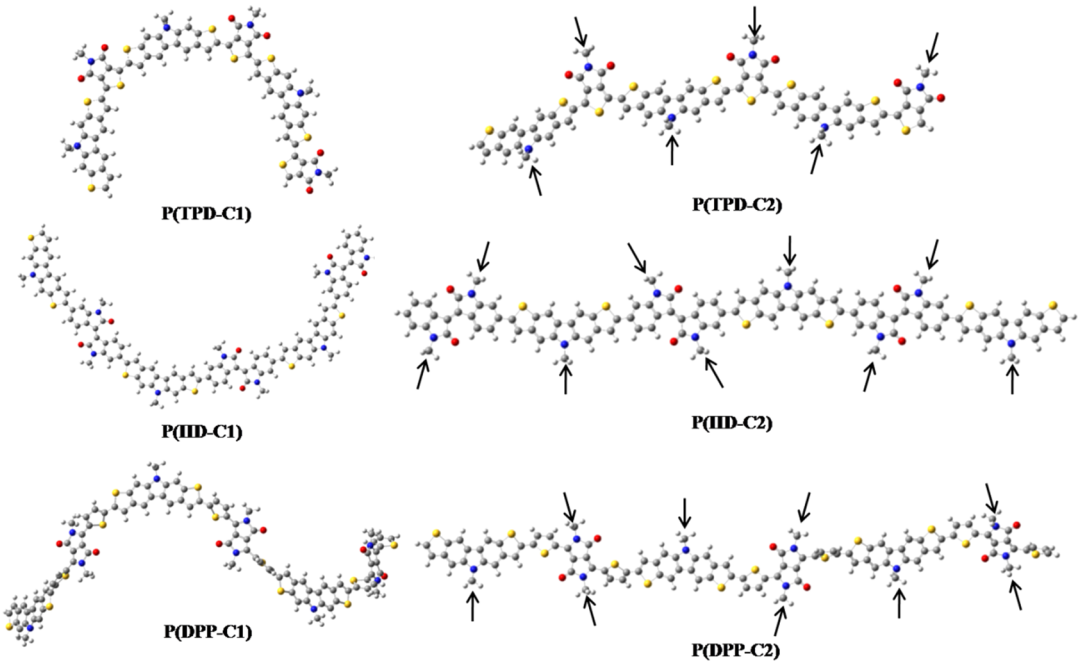

Figure 6. Optimized backbone conformation of the polymers. The side chains were replaced with methyl groups to simply the calculation. Arrows indicate the directions of the alkyl chains respective the polymer backbones.

19.9 Å. After thermal annealing, the diffraction peaks became stronger and sharper. This indicates that the films are out-of-plane ordered, and the polymer backbones adopt edge-on orientation respective to the substrates. However, SAED patterns of the films only showed diffraction rings at 7.6 and 9.0 Å for **P(TPD-C2)** and 7.5 Å for **P(DPP-C2)**, and no diffraction rings corresponding to π-stacking distance were observed. Considering the in-plane low order of the films, the field-effect mobilities of 0.31 and 1.36 $cm^2/(V\ s)$ for **P(TPD-C2)** and **P(DPP-C2)**, respectively, are pretty high, which can be attributed to the enhanced coplanarity of polymer backbones due to the introduction of large heteroacene unit **C2**.

To further understand the insight of the distinct semiconducting properties and film ordering structures of the polymers, the backbone conformation of the polymers was computationally optimized and is depicted in Figure 6. The polymers with **C1** as D-unit all have large backbone curvature, which may cause the difficult packing of the polymer chains, leading to the low-ordered films and thereby low mobility of their OFET devices. In contrast, the polymers with **C2** as D-unit display pseudo-straight-shaped backbones for **P(DPP-C2)** and **P(IID-C2)** and a sine-wave-shaped backbone for **P(TPD-C2)**. These results are consistent with the fact that the polymers based on **C2** have higher mobility than their counterparts based on **C1** unit. It is well-known that CPs with relatively straight backbones tends to form films with higher order, leading to higher mobility.[21,65] Note that the mobility of **P(IID-C2)** is much lower than that of **P(TPD-C2)**, **P(DPP-C2)**, and **IID**-based polymers with bithiophene as D unit (mobility is up to 2.48 $cm^2/(V\ s)$),[57−59] although it also has a relatively straight backbone. This may be attributed to the rigid nature of both **IID** and **C2** units, which results in highly stiff polymer backbone, prohibiting self-assembly of polymer chains even at high temperature. Moreover, alkyl chains on alternatively arranged D- and A-units of polymers **P(TPD-C2)**, **P(IID-C2)**, and **P(DPP-C2)** point to different directions (see arrows in Figure 6), which may also diminish the self-assembly ability of the polymers driven by interaction of alkyl chains, resulting in the low in-plane order of the films.

CONCLUSION

A series of donor−acceptor (D−A) CPs, i.e., **P(TPD-C1)**, **P(TPD-C2)**, **P(IID-C1)**, **P(IID-C2)**, **P(DPP-C1)**, and **P-(DDP-C2)** which contain isomeric dithienocarbazole units **C1** or **C2** as D-unit and **TPD**, **IID**, or **DPP** as A-unit, were synthesized, and their semiconducting properties were characterized with OFET devices. All polymers based on **C1** unit exhibited low mobility in the magnitude of 10^{-3} $cm^2/(V\ s)$ due to the low film order caused by their strong backbone curvature. In contrast, the polymers comprising **C2** unit have more straight backbones. However, **P(DPP-C2)** and **P(TPD-C2)** exhibited the highest mobility up to 1.36 and 0.31 $cm^2/(V\ s)$, respectively, while **P(IID-C2)** showed moderate mobility of 2.96×10^{-2} $cm^2/(V\ s)$. We attributed the low mobility of **P(IID-C2)** to its very stiff backbone, which results in poor self-assembly ability and therefore low-ordered film. Our results indicate that, for designing high mobility D−A CPs, structural units have to be appropriately selected to avoid the strong backbone curvature and meanwhile balance the intermolecular interaction and backbone stiffness.

EXPERIMENTAL SECTION

Instrumentation. ^1H and ^{13}C NMR spectra were recorded on a Bruker 300, 400, or 600 MHz spectrometer in $CDCl_3$. Chemical shift was reported relative to an internal tetramethylsilane (TMS) standard for the measurements with $CDCl_3$ as solvent. Elemental analysis was performed on a VarioEL elemental analysis system. TGA was carried out on a PerkinElmer TGA7 at a heating rate of 10 °C/min under nitrogen flow. DSC was performed on a PerkinElmer DSC 7 with a heating/cooling rate of ±10 °C/min under nitrogen flow. UV−vis absorption spectra were recorded on a Shimadzu UV-3600 UV−vis−NIR spectrometer. GPC analysis was conducted on a PL-GPC 220 system with polystyrene as standard and 1,2,4-trichlorobenzene as eluent at 150 °C or on a Waters 2414 system with polystyrene as

dx.doi.org/10.1021/ma301864f | *Macromolecules* XXXX, XXX, XXX−XXX

standard and tetrahydrofuran as eluent at 40 °C. E_g^{opt} was calculated according to the absorption onset of UV−vis−NIR absotption spectra (E_g^{opt} = 1240/λ_{onset} eV). Film CV was performed on a CHI660a electrochemical analyzer with a three-electrode cell at a scan rate of 100 mV/s in anhydrous acetonitrile. Bu_4NPF_6 (0.1 mol/L) was used as electrolyte. A glassy carbon electrode with a diameter of 10 mm, a Pt wire, and a saturated calomel electrode were used as the working, counter, and reference electrodes, respectively. HOMO and LUMO energy levels were estimated by the equations HOMO = −(4.80 + E_{onset}^{ox}) eV and LUMO = −(4.80 + E_{onset}^{re}) eV, in which E_{onset}^{ox} and E_{onset}^{re} are oxidation and reduction onsets in CV curves, respectively. Thin-film XRD was recorded on a Bruker D8 Discover thin-film diffractometer with Cu Kα radiation (λ = 1.540 56 Å) operated at 40 kV and 30 mA. Atomic force microscopy (AFM) measurements were performed in tapping mode on a SPA400HV instrument with a SPI 3800 controller (Seiko Instruments). SAED were taken on a JEOL JEM-1011 transmission electron microscope operated at an acceleration voltage of 100 kV with camera length of 160 cm and Au (111) diffraction as the external standard. Geometries of the polymer backbones were optimized based on semiempirical calculations using the Gaussian 03 package program. All alkyl substituents were replaced with methyl groups in order to simplify the calculations.

OFET Device Fabrication and Characterization. OFET devices were fabricated on heavily doped n-type silicon wafers with 300 nm thermally grown SiO_2 (C_i = 10 nF/cm^2). The substrate was first cleaned with acetone, methanol, and deionized water in an ultrasonic bath and then dried under a nitrogen flow, followed by heating at 100 °C for 30 min and a UV-zone treatment for 20 min. Then the substrate was modified by OTS-C8 according to ref 44. The polymer layer was deposited by spin-coating 6 mg/mL dichlorobenzene solution in ambient with 1200 rpm for 3 min. The resulting films were annealed at selected temperatures under nitrogen for 20 min. Finally, gold source and drain electrodes (40 nm) were evaporated on top through a shadow mask with a channel width (W) of 3000 μm and a channel length (L) of 100 μm. The electrical measurements were performed with two Keithley 236 source/measure units at room temperature in ambient. The mobility data were collected from more than five different devices.

■ ASSOCIATED CONTENT

Supporting Information

Synthetic details, DSC curves, and SAED patterns of the polymers. This material is available free of charge via the Internet at http://pubs.acs.org.

■ AUTHOR INFORMATION

Corresponding Author

*E-mail: yhgeng@ciac.jl.cn (Y.H.G.); xjzhang@ciac.jl.cn (X.J.Z.).

Notes

The authors declare no competing financial interest.

■ ACKNOWLEDGMENTS

This work is supported by National Basic Research Program of China (973 Project, No. 2009CB623603) of Chinese Ministry of Science and Technology, and National Science Foundation of China (Nos. 20921061 and 50833004).

■ REFERENCES

(1) Allard, S.; Forster, M.; Souharce, B.; Thiem, H.; Scherf, U. *Angew. Chem., Int. Ed.* **2008**, *47*, 4070.
(2) Guo, Y. L.; Yu, G.; Liu, Y. Q. *Adv. Mater.* **2010**, *22*, 4427.
(3) Wen, Y. G.; Liu, Y. Q. *Adv. Mater.* **2010**, *22*, 1331.
(4) Wang, C. L.; Dong, H. L.; Hu, W. P.; Liu, Y. Q.; Zhu, D. B. *Chem. Rev.* **2012**, *112*, 2208.
(5) Wen, Y. G.; Liu, Y. Q.; Gou, Y. L.; Yu, G.; Hu, W. P. *Chem. Rev.* **2011**, *111*, 3358.
(6) Arias, A. C.; MacKenzie, J. D.; McCulloch, I.; Rivnay, J.; Salleo, A. *Chem. Rev.* **2010**, *110*, 3.
(7) Thompson, B. C.; Fréchet, J. M. J. *Angew. Chem., Int. Ed.* **2008**, *47*, 58.
(8) Beaujuge, P. M.; Fréchet, J. M. J. *J. Am. Chem. Soc.* **2011**, *133*, 2009.
(9) Zhang, L.; Di, C.-A.; Yu, G.; Liu, Y. Q. *J. Mater. Chem.* **2010**, *20*, 7059.
(10) Ong, B. S.; Wu., Y. L.; Li, Y. N.; Liu, P.; Pan, H. L. *Chem.—Eur. J.* **2008**, *14*, 4766.
(11) Heeney, M.; Bailey, C.; Genevicius, K.; Shkunov, M.; Sparrowe, D.; Tierney, S.; McCulloch, I. *J. Am. Chem. Soc.* **2005**, *127*, 1078.
(12) McCulloch, I.; Heeney, M.; Bailey, C.; Genevicius, K.; Macdonald, I.; Shkunov, M.; Sparrowe, D.; Tierney, S.; Wagner, R.; Zhang, W.; Chabinyc, M. L.; Kline, R. J.; Mcgehee, M. D.; Toney, M. F. *Nat. Mater.* **2006**, *5*, 328.
(13) Li, Y. N.; Wu, Y. L.; Liu, P.; Birau, M.; Pan, H. L.; Ong, B. S. *Adv. Mater.* **2006**, *18*, 3029.
(14) Osaka, I.; Zhang, R.; Sauvé, G.; Smilgies, D.-M.; Kowalewski, T.; McCullough, R. D. *J. Am. Chem. Soc.* **2009**, *131*, 2521.
(15) Li, J.; Qin, F.; Li, C. M.; Bao, Q. L.; Chan-Park, M. B.; B. Zhang, W.; Qin, J. G.; Ong, B. S. *Chem. Mater.* **2008**, *20*, 2057.
(16) Pan, H. L.; Li, Y. N.; Wu, Y. L.; Liu, P.; Ong, B. S.; Zhu, S. P.; Xu, G. *J. Am. Chem. Soc.* **2007**, *129*, 4112.
(17) Liu, J. Y.; Zhang, R.; Sauvé, G.; Kowalewski, T.; McCullough, R. D. *J. Am. Chem. Soc.* **2008**, *130*, 13167.
(18) Rieger, R.; Beckmann, D.; Pisula, W.; Steffen, W.; Kastler, M.; Müllen, K. *Adv. Mater.* **2010**, *22*, 83.
(19) He, M. Q.; Li, J. F.; Sorensen, M. L.; Zhang, F. X.; Hancock, R. R.; R. Fong, H. H.; Pozdin, V. A.; Smilgies, D.-M.; Malliaras, G. G. *J. Am. Chem. Soc.* **2009**, *131*, 11930.
(20) Rieger, R.; Beckmann, D.; Pisula, W.; Kastler, M.; Müllen, K. *Macromolecules* **2010**, *43*, 6264.
(21) Osaka, I.; Abe, T.; Shinamura, S.; Tikimiya, K. *J. Am. Chem. Soc.* **2011**, *133*, 6852.
(22) Lin, C.-J.; Lee, W.-Y.; Liu, C.; Lin, H.-W.; Chen, W.-C. *Macromolecules* **2011**, *44*, 9565.
(23) Chen, Y. G.; Tian, H. K.; Yan, D. H.; Geng, Y. H.; Wang, F. S. *Macromolecules* **2011**, *44*, 5178.
(24) Chen, Y. G.; Liu, C. F.; Tian, H. K.; Bao, C.; Zhang, X. J.; Yan, D. H.; Geng, Y. H.; Wang, F. S. *Macromol. Rapid Commun.* **2012**, DOI: 10.1002/marc.201200330.
(25) Ding, P.; Chu, C.-C.; Liu, B.; Peng, B.; Zou, Y. P.; He, Y. H.; Zhou, K. C.; Hsu, C.-S. *Macromol. Chem. Phys.* **2010**, *211*, 2555.
(26) Fei, Z. P.; Kim, J. S.; Smith, J.; Domingo, E. B.; Anthopoulos, T. D.; Stingelin, N.; Watkins, S. E.; Kim, J.-S.; Heeney, M. *J. Mater. Chem.* **2011**, *21*, 16257.
(27) Ong, K.-H.; Lim, S.-L.; Tan, H.-S.; Wong, H.-K.; Li, J.; Ma, Z.; Moh, L. C. H.; Lim, S.-H.; de, Mello, J. C.; Chen, Z.-K. *Adv. Mater.* **2011**, *23*, 1409.
(28) Yuen, J. D.; Kumar, R.; Zakhidov, D.; Seifter, J.; Lim, B.; Heeger, A. J.; Wudl, F. *Adv. Mater.* **2011**, *23*, 3780.
(29) Cripin, X.; Chen, M. X.; Perzon, E.; Anderson, M. R.; Pullerits, T.; Andersson, M.; Inganäs, O.; Berggren, M. *Appl. Phys. Lett.* **2005**, *87*, 252105.
(30) Fan, J.; Yuen, J. D.; Wang, M. F.; Seifter, J.; Seo, J.-H.; Mohebbi, A. R.; Zakhidov, D.; Heeger, A. J.; Wudl, F. *Adv. Mater.* **2012**, *24*, 2186.
(31) Zhang, W. M.; Smith, J.; Watkins, S. E.; Gysel, R.; McGehee, M.; Salleo, A.; Kirkpatricki, J.; Ashraf, S.; Anthopoulos, T.; Heeney, M.; McCulloch, I. *J. Am. Chem. Soc.* **2010**, *132*, 11437.
(32) Ying, L.; Hsu, B. B. Y.; Zhan, H. M.; Welch, G. C.; Zalar, P.; Perez, L. A.; Kramer, E. J.; Nguyen, T.-Q.; Heeger, A. J.; Wong, W.-Y.; Bazan, G. C. *J. Am. Chem. Soc.* **2011**, *133*, 18538.
(33) Osaka, I.; Shimawaki, M.; Mori, H.; Doi, I.; Miyazaki, E.; Koganezawa, T.; Takimiya, K. *J. Am. Chem. Soc.* **2012**, *134*, 3498.
(34) Guo, X. G.; Ortiz, R. P.; Zheng, Y.; Kim, M.-G.; Zhang, S. M.; Hu, Y.; Lu, G.; Facchetti, A.; Marks, T. J. *J. Am. Chem. Soc.* **2011**, *133*, 13685.

(35) Osaka, I.; Takimiya, K.; McCullough, R. D. *Adv. Mater.* **2010**, *22*, 4993.
(36) Kim, D. H.; Lee, B.-L.; Moon, H.; Kang, H. M.; Jeong, E. J.; Park, J-II.; Han, K.-M.; Lee, S.; Yoo, B. W.; Koo, B. W.; Kim, J. Y.; Lee, W. H.; Cho, K.; Beceril, H. A.; Bao, Z. N. *J. Am. Chem. Soc.* **2009**, *131*, 6124.
(37) Osaka, I.; Sauvé, G.; Zhang, R.; Kowalewski, T.; McCullough, R. D. *Adv. Mater.* **2007**, *19*, 4160.
(38) Liu, J. Y.; Zhang, R.; Osaka, I.; Mishra, S.; Javier, A. E.; Smilgies, D.-M.; Kowalewski, T.; McCullough, R. D. *Adv. Funct. Mater.* **2009**, *19*, 3427.
(39) Osaka, I.; Zhang, R.; Sauvé, G.; Smilgies, D.-M.; Kowalewski, T.; McCullough, R. D. *J. Am. Chem. Soc.* **2009**, *131*, 2521.
(40) Zhang, M.; Tsao, H. N.; Pisula, W.; Yang, C.; Mishra, A. K.; Müllen, K. *J. Am. Chem. Soc.* **2007**, *129*, 3472.
(41) Wang, S. H.; Kappl, M.; Liebewirth, I.; Müller, M.; Kirchhoff, K.; Pisula, W.; Müllen, K. *Adv. Mater.* **2012**, *24*, 417.
(42) Tsao, H. N.; Cho, D. M.; Park, I.; Hansen, M. R.; Mavrinskiy, A.; Yoon, D. Y.; Graf, R.; Pisula, W.; Spiess, H. W.; Müllen, K. *J. Am. Chem. Soc.* **2011**, *133*, 2605.
(43) Zhang, X. R.; Richter, L. J.; DeLongchamp, D. M.; Kline, R. J.; Hammond, M. R.; McCulloch, I.; Heeney, M.; Ashraf, R. S.; Smith, J. N.; Anthopoulos, T. D.; Schroeder, B.; Geerts, Y. H.; Fischer, D. A.; Toney, M. F. *J. Am. Chem. Soc.* **2011**, *133*, 15073.
(44) Li, Y. N.; Sonar, P.; Singh, S. P.; Soh, M. S.; van Meurs, M.; Tan, J. *J. Am. Chem. Soc.* **2011**, *133*, 2198.
(45) Li, Y. N.; Singh, S. P.; Sonar, P. *Adv. Mater.* **2010**, *22*, 4862.
(46) Jung, J. W.; Liu, F.; Russell, T. P.; Jo, W. H. *Energy Environ. Sci.* **2012**, *5*, 6857.
(47) Bronstein, H.; Chen, Z. Y.; Ashraf, R. S.; Zhang, W. M.; Du, J. P.; Durrant, J. R.; Tuladhar, P. S.; Song, K.; Watkins, S. E.; Geerts, Y.; Wienk, M. M.; Janssen, R. A. J.; Anthopoulos, T.; Sirringhaus, H.; Heeney, M.; McCulloch, I. *J. Am. Chem. Soc.* **2011**, *133*, 3272.
(48) Wu, P.-T.; Kim, F. S.; Jenekhe, S. A. *Chem. Mater.* **2011**, *23*, 4618.
(49) Sonar, P.; Singh, S. P.; Li, Y. N.; Ooi, Z.-E.; Ha, T.-J.; Wong, I.; Soh, M. S.; Dodabalapur, A. *Energy Environ. Sci.* **2011**, *4*, 2288.
(50) Ashraf, R. S.; Chen, Z. Y.; Leem, D. S.; Bronstein, H.; Zhang, W. M.; Schroeder, B.; Geerts, Y.; Smith, J.; Watkins, S.; Anthopoulos, T. D.; Sirringhaus, H.; de Mello, J. C.; Heeney, M.; McCulloch, I. *Chem. Mater.* **2011**, *23*, 768.
(51) Shahid., M.; McCarthy-Ward, T.; Labram, J.; Rossbauer, S.; Domingo, E. B.; Watkins, S. E.; Stingelin, N.; Anthopoulos, T. D.; Heeney, M. *Chem. Sci.* **2012**, *3*, 181.
(52) Lin, H.-W.; Lee, W.-Y.; Chen, W.-C. *J. Mater. Chem.* **2012**, *22*, 2120.
(53) Li, Y. N.; Sonar, P.; Singh, S. P.; Zeng, W. J.; Soh, M. S. *J. Mater. Chem.* **2011**, *21*, 10829.
(54) Sonar, P.; Singh, S. P.; Li, Y. N.; Soh, M. S.; Dodabalapur, A. *Adv. Mater.* **2010**, *22*, 5409.
(55) Lee, J. S.; Son, S. K.; Song, S.; Kim, H.; Lee, D. R.; Kim, K.; Ko, M. J.; Choi, D. H.; Kim, B.; Cho, J. H. *Chem. Mater.* **2012**, *24*, 1316.
(56) Chen, H. J.; Cuo, Y. L.; Yu, G.; Zhao, Y.; Zhang, J.; Gao, D.; Liu, H. T.; Liu, Y. Q. *Adv. Mater.* **2012**, *24*, 4618.
(57) Lei, T.; Cao, Y.; Fan, Y. L.; Liu, C.-J.; Yuan, S.-C.; Pei, J. *J. Am. Chem. Soc.* **2011**, *133*, 6099.
(58) Lei, T.; Cao, Y.; Zhou, X.; Peng, Y.; Bian, J.; Pei, J. *Chem. Mater.* **2012**, *24*, 1762.
(59) Mei, J. G.; Kim, D. H.; Ayzner, A. L.; Toney, M. F.; Bao, Z. N. *J. Am. Chem. Soc.* **2011**, *133*, 20130.
(60) Cheng, Y.-J.; Wu, J.-S.; Shih, P.-I.; Chang, C.-Y.; Jwo, P.-C.; Kao, W.-S.; Hsu, C.-S. *Chem. Mater.* **2011**, *23*, 2361.
(61) Zhang, M. J.; Guo, X.; Wang, X. C.; Wang, H. Q.; Li, Y. F. *Chem. Mater.* **2011**, *23*, 4264.
(62) Wu, J.-S.; Cheng, Y.-J.; Lin, T.-Y.; Chang, C.-Y.; Shih, P.-I.; Hsu, C.-S. *Adv. Funct. Mater.* **2012**, *22*, 1711.
(63) Johansson, T.; Mammo, W.; Svensson, M.; Andersson, M. R.; Inganäs, O. *J. Mater. Chem.* **2003**, *13*, 1316.
(64) Bard, A.; Faulkner, L. A. *Electrochemical Methods – Fundamentals and Applications*; Wiley: New York, 1984.
(65) Rieger, P.; Beckmann, D.; Mavrinskiy, A.; Kastler, M.; Müllen, K. *Chem. Mater.* **2010**, *22*, 5314.